Water Research 252 (2024) 121247

Contents lists available at ScienceDirect

Water Research

journal homepage: www.elsevier.com/locate/watres

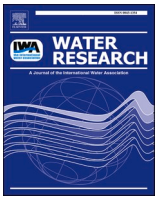

Prioritizing ecological restoration in hydrologically sensitive areas to improve groundwater quality

Yao Wang [a,b], Yiqi Yu [a,b], Xin Luo [c,d], Qiaoguo Tan [a,b], Yuqi Fu [a,b], Chenhe Zheng [b,e], Deli Wang [b,e,*], Nengwang Chen [a,b,*]

[a] Fujian Provincial Key Laboratory for Coastal Ecology and Environmental Studies, College of the Environment and Ecology, Xiamen University, Xiamen, China
[b] State Key Laboratory of Marine Environmental Science, Xiamen University, Xiamen, China
[c] Department of Earth Sciences, The University of Hong Kong, Hong Kong, China
[d] Shenzhen Research Institute (SRI), The University of Hong Kong, Shenzhen, China
[e] College of Ocean and Earth Science, Xiamen University, Xiamen, China

ARTICLE INFO

Keywords:
Land use
Hydrological connectivity
Nutrients
Heavy metals
Water quality management

ABSTRACT

Greening is the optimal way to mitigate climate change and water quality degradation caused by agricultural expansion and rapid urbanization. However, the ideal sites to plant trees or grass to achieve a win–win solution between the environment and the economy remain unknown. Here, we performed a nationwide survey on groundwater nutrients (nitrate nitrogen, ammonia nitrogen, dissolved reactive phosphorus) and heavy metals (vanadium, chromium, manganese, iron, cobalt, nickel, copper, arsenic, strontium, molybdenum, cadmium, and lead) in China, and combined it with the global/national soil property database and machine learning (random forest) methods to explore the linkages between land use within hydrologically sensitive areas (HSAs) and groundwater quality from the perspective of hydrological connectivity. We found that HSAs occupy approximately 20 % of the total land area and are hotspots for transferring nutrients and heavy metals from the land surface to the saturated zone. In particular, the proportion of natural lands within HSAs significantly contributes 8.0 % of the variability in groundwater nutrients and heavy metals in China ($p < 0.01$), which is equivalent to their contribution (8.8 %) at the regional scale (radius = 4 km, area = 50 km^2). Increasing the proportion of natural lands within HSAs improves groundwater quality, as indicated by the significant reduction in the concentrations of nitrate nitrogen, manganese, arsenic, strontium, and molybdenum ($p < 0.05$). These new findings suggest that prioritizing ecological restoration in HSAs is conducive to achieving the harmony between the environment (improving groundwater quality) and economy (reducing investment in area management).

1. Introduction

To mitigate the effects of global climate change, China proposed the "3060″ goals for peaking carbon dioxide emissions by 2030 and achieving carbon neutrality by 2060 (China updated nationally determined contributions, 2021). Thus, a series of ecological restoration and protection measures are undergoing to realize these goals (Liu et al., 2021). For decades, the afforestation (or “Grain for Green”) program has been one of the important measures of ecological governance in China (Deng et al., 2017). In fact, China is the global leads in greening (Li et al., 2018), contributing 25 % of the global net increase in leaf area via only 6.6 % of the global vegetation area (Chen et al., 2019). Since national investment in ecological restoration is not limitless, policy–makers need to identify priority planting areas to maximize ecological benefits (Ge et al., 2023).

For a long time, groundwater quality in China and around the world has faced great challenges from overloads of nutrients and heavy metals (Gu et al., 2013; Li et al., 2023; Mitchell et al., 2011). Previous studies have shown that groundwater quality is significantly affected by land uses and hydrogeological properties (Liang et al., 2022; Kellner et al., 2015; Fatichi et al., 2020). Land use/cover change (e.g., agricultural expansion and rapid urbanization) is thought to be the main cause of groundwater nutrient overload (Gu et al., 2013; Basu et al., 2022; McDonough et al., 2020; Schilling et al., 2015). Groundwater heavy metal concentrations are also generally affected by human activities in land surfaces, such as wastewater irrigation (Yang et al., 2021),

* Corresponding authors.
E-mail addresses: deliwang@xmu.edu.cn (D. Wang), nwchen@xmu.edu.cn (N. Chen).

https://doi.org/10.1016/j.watres.2024.121247
Received 18 July 2023; Received in revised form 18 January 2024; Accepted 31 January 2024
Available online 1 February 2024

fertilization (Fan et al., 2022), and pesticide application (Xu et al., 2019). Pollutants are usually transported from the land surface to the saturated zone via hydrological connections (Leibowitz et al., 2023; Vereecken et al., 2022; Yue et al., 2023), but are controlled by hydrogeological properties (Fatichi et al., 2020). The high porosity or high soil saturated hydraulic conductivity (Ksat) of sandy soil is conducive to the vertical migration of pollutants under hydrological connections, but the opposite is true for clay soil (Zhu et al., 2018; Gupta et al., 2021). Moreover, the soil structure influences both hydrological connectivity and the material cycle, by changing the soil water capacity or availability, adsorption/desorption processes and redox conditions (Fatichi et al., 2020; Zhu et al., 2018) and further affects groundwater quality. Previous researchers have reported the positive effects of ecological restoration (e.g., afforestation and grass planting) on groundwater quality (Kellner et al., 2015). However, the ideal sites to plant trees or grass to obtain high ecological benefits (especially for improving groundwater quality) with low investment costs remain largely unknown.

Hydrologically sensitive areas (HSAs) refer to the soils in the landscape most likely subject to runoff under saturation (Thomas et al., 2016). They usually occupy only approximately 20 % of the total watershed area but have high hydrological connectivity affecting the migration and transformation of pollutants (Anderson et al., 2015; Wang et al., 2023). Previous studies showed that river pollutant concentrations could be greatly reduced by increasing the proportion of forestland within HSAs (Giri et al., 2017; Zhou et al., 2022; Wang et al., 2023). This highlighted that HSAs have strong connectivity and are considered as hotspots for hydrological activities in horizontal direction (Qiu et al., 2019). Hydrological connectivity is also commonly manifested in vertical leaching and long–distance transport of saturated soil water (Yue et al., 2023; Jiang et al., 2019; Zhu et al., 2018). However, there are still limited reports on the effects of greening in HSAs on groundwater quality, especially at a national scale. This is mainly due to the difficulty in determining the spatial distribution of actual soil Ksat. Ksat usually controls the allocation among precipitation, infiltration, and runoff (Gupta et al., 2021) and is also an essential parameter to constrain the spatial distribution of HSAs (Qiu et al., 2019). Recently, the development of a global database for Ksat (Gupta et al., 2021) and the widespread use of machine learning methods (Koch et al., 2019; Li et al., 2017; Knoll et al., 2020) have provided convenience for the spatial extrapolation of Ksat at a large scale. Given the potential of HSAs in characterizing hydrological connectivity (Giri et al., 2018; Thomas et al., 2016), we speculate that ecological restoration in HSAs could be beneficial in improving the groundwater quality at national scale.

We therefore performed a nationwide groundwater quality survey (specifically for nutrients and heavy metals) and delineated regional HSAs across the country. The main objectives of this study are to explore the relationship between land uses within HSAs and groundwater quality, and further discuss the feasibility of ecological restoration in HSAs to achieve a win–win solution between the environment (improving groundwater quality) and the economy (reducing investment in area management).

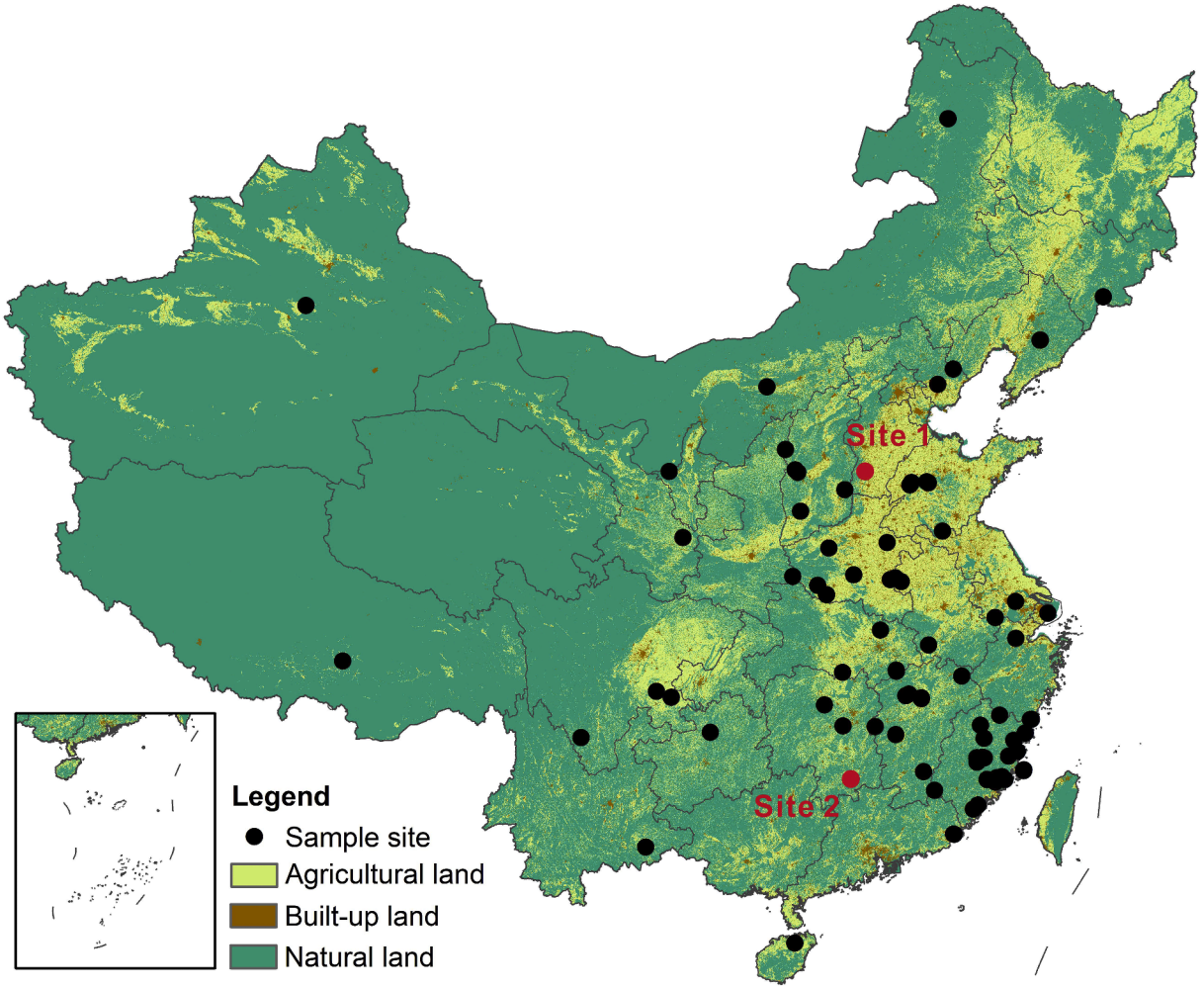

Fig. 1. Spatial distribution of groundwater sampling sites (n = 90) and land uses in China.

2. Materials and methods

2.1. Nation–wide survey on groundwater nutrients and heavy metals

In this study, a total of 90 groundwater samples were collected based on the Undergraduate Winter Practice Program of Xiamen University in 2016 ($n = 55$), 2018 ($n = 13$) and 2019 ($n = 22$). These sampling sites cover 25 (74 %) provincial–level administrative regions in China (Fig. 1). The water samples were obtained from 89 domestic wells (sampling depth ranging from 2 to 200 m) and 1 spring. Approximately 0.5 L of groundwater was collected into a clean polyvinyl chloride bottle, sealed with plastic film. All the samples were transported to the laboratory for further analysis under cold–chain logistics.

Groundwater samples were filtered through GF/F membranes for nutrient analysis. The concentrations of dissolved nutrients (nitrate nitrogen, NO_3–N; ammonia nitrogen, NH_4–N; dissolved reactive phosphorus, DRP) were determined using segmented flow automated colorimetry (San++ analyser, Germany). The concentrations of heavy metals (vanadium, V; chromium, Cr; manganese, Mn; iron, Fe; cobalt, Co; nickel, Ni; copper, Cu; arsenic, As; strontium, Sr; molybdenum, Mo; cadmium, Cd; lead, Pb) in groundwater were determined by ICP–MS (Agilent 7700) according to the method of Wang et al. (2012).

2.2. Extrapolation of Ksat by the random forest model

The SoilKsatDB (a global Ksat database) comprises 13,258 Ksat measurements from 1,908 sites collected from the published literature and other sources (Gupta et al., 2021). Here, we used the SoilKsatDB combined with a machine learning model (random forest, RF) to construct the RF model between Ksat and environmental variables. Furthermore, based on the constructed RF model, we extrapolated the spatial distribution of Ksat in China. Considering the feasibility of the extrapolation method, only environmental variables appearing in both Chinese national databases and SoilKsatDB were used for modelling, i.e., clay, silt, sand, bulk density (BD), and soil organic carbon (SOC). These soil properties have a strong influence on the hydrological process in terrestrial systems (Zhu et al., 2018) and were therefore selected for Ksat modelling. The details for all data are given in Table S1.

The RF model is a machine learning algorithm based on an enhanced utilization of classification or regression trees, which was first proposed by Breiman (2001). It is a nonparametric multivariate modelling technique, with good performance in capturing nonlinear dependence (Koch et al., 2019). Because the RF model does not assume any probability distribution for the data, no overfitting problem occurs as the number of trees increases (Li et al., 2017). The RF model, as a powerful tool, is widely used to evaluate the spatial distribution of geochemical parameters from regional (He et al., 2022) to national (Koch et al., 2019) scale.

In the present study, a five–fold cross validation method was used to construct the RF model. It usually divides all data into five equal parts, four for training and one for testing. The five rounds of training and testing ensure that all data can be used in the construction of the RF model. The advantage of this approach is that it ensures that the final model can be evaluated by an average result of five training and testing runs. To better identify important environmental variables for predicting Kast, we constructed 31 RF models considering all combinations between Ksat and five environmental variables (soil clay, silt, sand, BD, and SOC) (Table S2). Here, the RF model followed the default parameter settings. For the best–performing RF model, we further adjusted the four main parameters to improve the simulation accuracy using GridSearchCV (a Python package from sklearn.model_selection). The four main parameters include [n_estimators], [min_samples_split], [min_samples_leaf], and [max_depth]. These parameters generally control the structure of trees in the RF model, as described in detail in Table S3. Moreover, the influence of environmental variables on the prediction results in the best–performing RF model was explored by SHapley Additive exPlanations (SHAP) analysis and shown in Fig. S1. SHAP analysis is a post–hoc explanation method based on the ideas of game theory, which can decompose global predictions into additive contributions of local features, keeping the global and local explanations consistent (Li et al., 2022). The importance of environmental variables can be ranked according to the magnitude of the mean absolute SHAP value (Wang et al., 2022).

The RF model performance was evaluated based on three objective functions, including the root mean squared error (RMSE), the Nash–Sutcliffe efficiency (NSE) and the coefficient of determination (R^2). A satisfactory RF model usually has a RMSE approximating zero and both NSE and R^2 close to one. Lastly, we finally estimated the spatial distribution of Ksat in China using the RF model with the best simulation accuracy (Fig. 2).

2.3. Soil topographic index

The soil topographic index (STI) method can assess the probability of saturated excess runoff at a landscape location by considering spatial variations in hydrologically related soil properties (Qiu et al., 2019). The STI can be calculated using the following equation (Giri et al., 2017):

$$\mathrm{STI} = \ln(\alpha/\tan\beta) - \ln(\mathrm{Ksat} \times D) \quad (1)$$

where ln (α/tanβ) is the topographic wetness index (TWI), which indicates the control of soil moisture saturation by topographic features at different landscape positions. Here, α is the upslope area per unit contour length (m), and β is the topographic slope (mm^{-1}). The TWI is calculated based on a digital elevation model (DEM) with 30 m spatial resolution (Geospatial Data Cloud, http://www.gscloud.cn/). The ln (Ksat × D) term represents the soil transmissivity. Ksat is the soil saturated hydraulic conductivity (m d^{-1}), which is extrapolated based on the RF model in Section 2.2. D is the soil thickness above the restrictive layer (m). The data sources are listed in Table S1.

2.4. Hydrologically sensitive areas

A high STI value usually indicates a strong tendency toward runoff production and contaminant transfer (Thomas et al., 2016). Previous studies have reported that the STI threshold method can be used to delineate HSAs (Giri et al., 2018; Qiu et al., 2019). In the method, a predetermined STI threshold is selected, and the areas where the STI value is greater than the threshold are identified as HSAs. This approach typically focuses on the areas with high STI values that comprise 20 % of the total area (Giri et al., 2017; Zhou et al., 2022). The current study delineated the HSAs using an STI threshold value of 10. A higher STI threshold is usually associated with a smaller area of HSAs (Giri et al., 2018). The spatial distribution of HSAs is presented in Fig. 2.

2.5. Land use at HSA and regional scales

In typical irrigated agricultural areas, approximately 7 observation wells are usually set up within 100 km^2 for monitoring agricultural pollution, and one monitoring well is set up per an average of 14 km^2 (China technical specifications for environmental monitoring of groundwater, HJ 164–2020). To better explore the relationship between land use and groundwater quality, a total of 4 concentric circles with different radii ($r = 1$, 2, 3 and 4 km, respectively; area= 3, 13, 28 and 50 km^2, respectively) centred around the sampling site were set up to extract land use at both the HSA and regional scale. The land use map (2018 year) with a spatial resolution of 30 m was obtained from the Data Center for Resources and Environmental Sciences, Chinese Academy of Sciences (RESDC) (http://www.resdc.cn). Land uses were reclassified into three categories, including agricultural land, built–up land and natural land (30 % forestland, 36 % grassland, 30 % unused land, and the rest was water). The spatial distribution of land use is shown in Fig. 1.

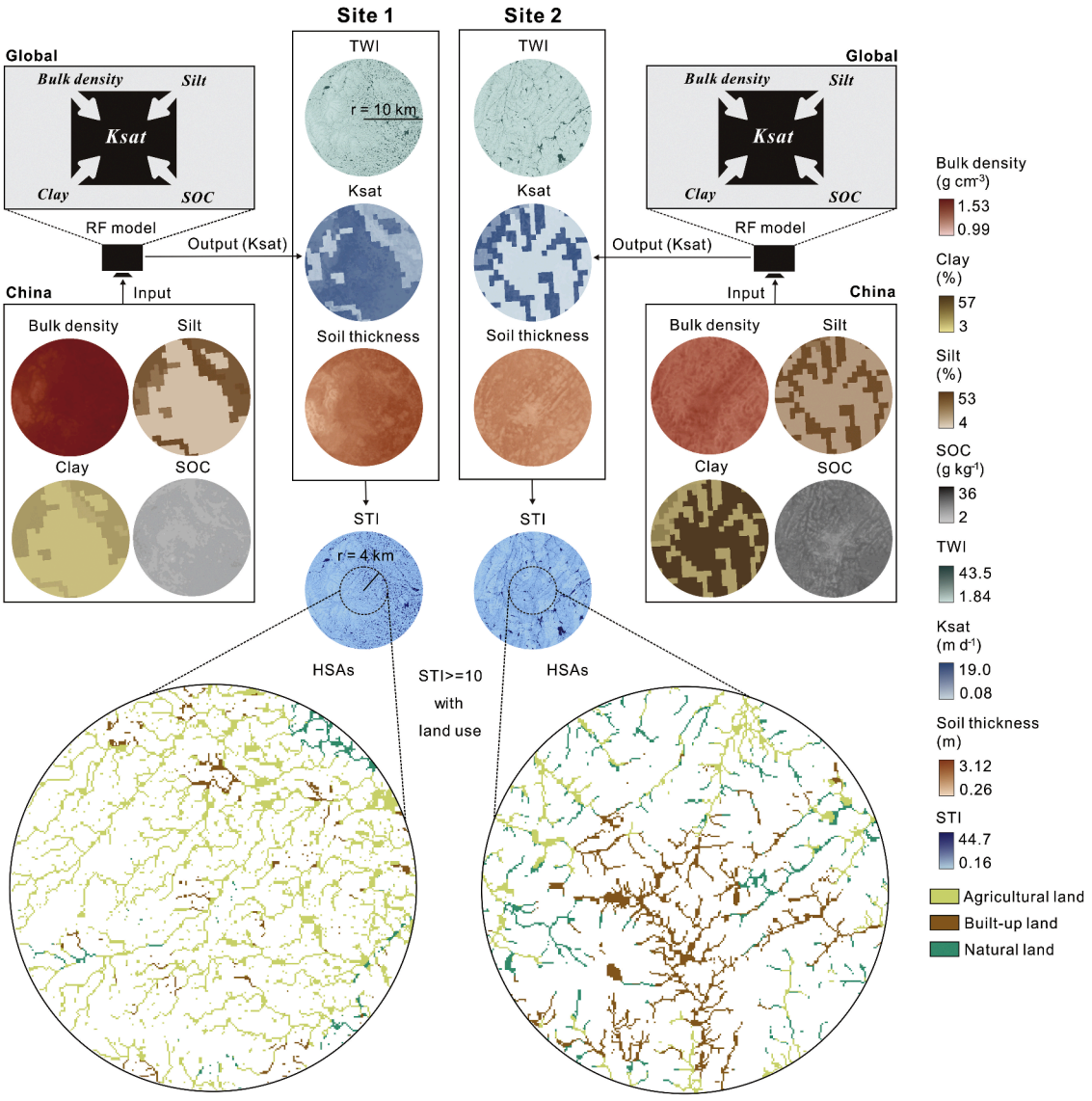

Fig. 2. Two examples (site 1 and site 2) of the extraction of both hydrologically sensitive areas (HSAs) and their land use. Here, we first constructed a random forest (RF) model between soil saturated hydraulic conductivity (Ksat) and environmental variables (bulk density, clay, silt, and soil organic carbon) based on a global database (see Section 2.2). Then, we extrapolated the spatial distribution of Ksat in China through the established RF model combined with the soil property database of China. Finally, we calculated the spatial distribution of HSAs at the 90 sampling sites based on Eq. (1), and further overlaid land use with HSAs. The locations of both site 1 and site 2 are shown in Fig. 1. The ranges of STI values based on a total of 90 circular areas (each circular area= 50 km^2; r = 4 km). SOC, soil organic carbon. TWI, topographic wetness index. STI, soil topographic index.

2.6. Statistical analysis

The *t*–test was used to assess the differences in groundwater nutrient and heavy metal concentrations between different sampling depths. Spearman rank correlation and linear regression analysis were conducted using SPSS software (version 19.0) to determine the relationship between land uses and groundwater nutrient (or heavy metal) concentrations at both the regional and HSA scales. Before regression analysis, all data were logarithmically transformed to satisfy the comparability of models at different scales and avoid the impacts of data skewness (Giri et al., 2018). Four main evaluation parameters were used to determine the model performance at different scales, including the adjusted R^2, Akaike information criterion (AIC), Bayesian information criterion (BIC) and log–likelihood. Usually, a higher adjusted R^2 and log–likelihood but lower AIC and BIC indicate an optimal model.

Redundancy analysis (RDA) is a multivariate direct gradient analytical method and a form of principal component analysis performed under the constraint of environmental factors (Xie et al., 2021; Wang et al., 2023). RDA can well reflect the relationship between target variables and environmental factors and identify factors with significant contributions (Tang et al., 2023; Jiang et al., 2019). In the present study, we used RDA to explore the contribution of land use to groundwater quality at the regional and HSA scales. The statistical significance was tested by a Monte Carlo permutation method based on 999 runs with randomized data. RDA was performed in Canoco for Windows software (version 5.0).

3. Results and discussion

3.1. Spatial characteristics of land use within HSAs

The Ksat map is an important component in the workflow of calculating HSAs (Fig. 2). It describes the rate of water movement, which is a key variable affecting the transfer of pollutants in both the horizontal

and vertical directions (Gupta et al., 2021). However, the spatial distribution of soil properties is usually difficult to obtain at large scales with high spatial resolution (Vereecken et al., 2022). Here, we used the global Ksat database (Gupta et al., 2021) combined with the RF model (Breiman, 2001) to extrapolate the distribution of Ksat in China (Fig. 2). A total of 31 RF models were constructed to determine the optimal combination of parameters for modelling (Table S2). The parameters of BD, clay, silt, and SOC were identified as the best combination to construct the RF model, which exhibited the highest R^2 and NSE but the lowest RMSE in the test sets. After optimizing the model parameters (Table S3), the R^2 and NSE increased to 0.610 and 0.600 respectively, while RMSE is lowered to 0.638 m d^{-1} in independent test sets (Fig. 3). Soil clay had the greatest contribution to Ksat prediction in the RF model, followed by BD, silt and SOC based on the mean absolute SHAP value (Fig. S1). Overall, the model performances in all aspects were higher than those of other RF models applied at regional (Li et al., 2017) and national (Knoll et al., 2020; Koch et al., 2019) scales. We finally used the constructed RF model and combined it with the Chinese database (maps of BD, clay, silt, and SOC) to extrapolate the Ksat map and implement the spatial computation of STI in China (Fig. 2).

In the present study, the STI ranged from 0.16 to 44.7 within 90 circular areas with each area being 50 km^2 (Fig. 2). A STI threshold value of 10 was used to obtain the HSAs that accounted for 20.8 % of the total circular areas (Fig. S2). Furthermore, we obtained the composition of land use within HSAs by superimposing both HSAs and land use (Fig. 4). We found that with the expansion of circular areas, agricultural land always maintained a stable and large proportion. This showed that human modification of the land surface was centred around agriculture, while the use of agricultural fertilizers and pesticides greatly increased the risk of water pollution (Winkler et al., 2021; Xu et al., 2019; Gu et al., 2013). We also found that the spatial composition of land use within HSAs was similar to that at the regional scale (Fig. 4). HSAs usually have strong hydrological connectivity to transfer pollutants into the water environment (Giri et al., 2018). Therefore, high–intensity human activities within HSAs could aggravate the degradation of river and groundwater quality (Wang et al., 2023).

3.2. *Effect of land use within HSAs on groundwater nutrients and heavy metals*

We investigated the concentrations of nutrients and heavy metals in groundwater at 90 sites across the country. Descriptive statistics for the groundwater nutrient and heavy metal parameters at the total and different sampling depths can be found in Tables S4 and S5, respectively. Overall, all groundwater parameters presented high spatial variability. This may be attributed to the high environmental heterogeneity across the national scale, e.g., topography and hydrology (Jarsjo et al., 2020; Li et al., 2020; Scanlon et al., 2022). A significant positive correlation was found between groundwater parameters (nutrients and heavy metals) (Fig. S3). This implies that they may show similar behaviour characteristics when migrating from the land surface to the saturated zone. We further found that high rainfall and steep slopes are generally associated with low concentrations of most groundwater nutrient and heavy metal parameters, but with high concentrations of groundwater DRP ($p < 0.01$) and Cd ($p < 0.05$) (Fig. S3). This may be attributed to the activation of hydrological connectivity in the soil system by rainfall, especially at steep slopes (usually with high groundwater flow rates), which exacerbate nutrient loss and pollutant migration (Giri et al., 2018; Li et al., 2020; Zhu et al., 2018). Some studies have shown that extreme rainstorm events facilitate the transfer of land matter from the surface to the deep soil or saturated zone (Mihiranga et al., 2021; Mo et al., 2022). The above results indicate that the behaviour characteristics of nutrients and heavy metals entering groundwater are generally highly responsive to regional hydrological connectivity. This implies that the HSAs that are most likely to produce runoff may also be the critical areas for the vertical migration of nutrients and heavy metals.

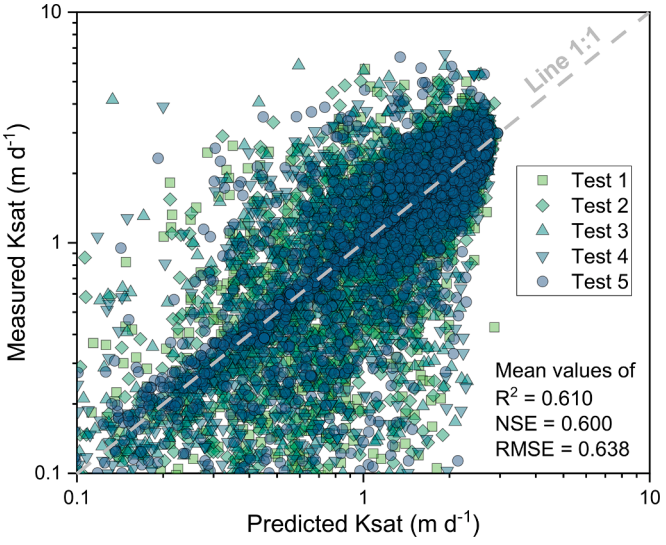

Fig. 3. Results of the random forest model for soil saturated hydraulic conductivity (Ksat) after adjusting parameters using five–fold cross validation in the independent test sets (each test, n = 1,812). R^2, the coefficient of determination. NSE, Nash–Sutcliffe efficiency. RMSE, root mean squared error.

It is difficult for humans to directly change regional topography and rainfall conditions to control the vertical transport of pollutants and reduce groundwater pollution. Considering that the sources of both nutrients and heavy metals in groundwater mainly come from human activities on land surfaces (Gu et al., 2013; Yang et al., 2021; Yuan et al., 2020), while land use is a comprehensive reflection of human activities (Winkler et al., 2021). Thus, changing land uses within HSAs based on hydrological connectivity may be a feasible approach to achieve an ideal groundwater quality. In the present study, at the HSA scale, groundwater nutrient and heavy metal concentrations were positively correlated with both agricultural land and built–up land but negatively correlated with natural land (Fig. S4). This suggests that human activities (e.g., agricultural expansion and rapid urbanization) significantly elevate groundwater nutrients and heavy metals (Yang et al., 2021; Yuan et al., 2020), but natural land has a profound impact on the purification of the water environment (Giri et al., 2018). Generally, at the HSA scale, natural land contributes 8.0 % ($p < 0.01$) of the variation to all groundwater parameters, while agricultural land contributes 6.4 % ($p < 0.01$) of the variation (Fig. 5). The low but significant contribution rate may be attributed to the small sample size and complex environment at a national scale (Scanlon et al., 2022). Notably, the contribution rate of natural land on groundwater quality at the HSA scale is basically consistent with that at the regional scale (Fig. 5). This result is the same for the different sampling years (Table S6). These findings also support that HSAs are hotspot areas affecting groundwater quality in China.

Land surface pollutants tend to contaminate groundwater through both vertical leaching and long–distance transport under the dynamics of subsoil and groundwater hydrology (Zhu et al., 2018). Therefore, we further constructed regression models under different sampling radii at different scales to explore the effective radius for performing ecological restoration to significantly improve groundwater quality (Table S7). For both natural land and groundwater parameters (NO_3–N, Mn, As, Sr, and Mo), a negligible difference was found in the model slope, significance level, adjusted R^2, AIC, BIC, and log–likelihood at both the regional and HSA scales. This suggests that the effectiveness of ecological restoration on groundwater improvement at the HSA scale is equivalent to that at the regional scale. This further demonstrates the potential of increasing the proportion of natural land in HSAs to improve groundwater quality. From the perspective of distance at both the regional and HSA scales, groundwater quality (Mn, As, Sr, and Mo) can be significantly improved by increasing the proportion of natural land within a radius of 1 km, but

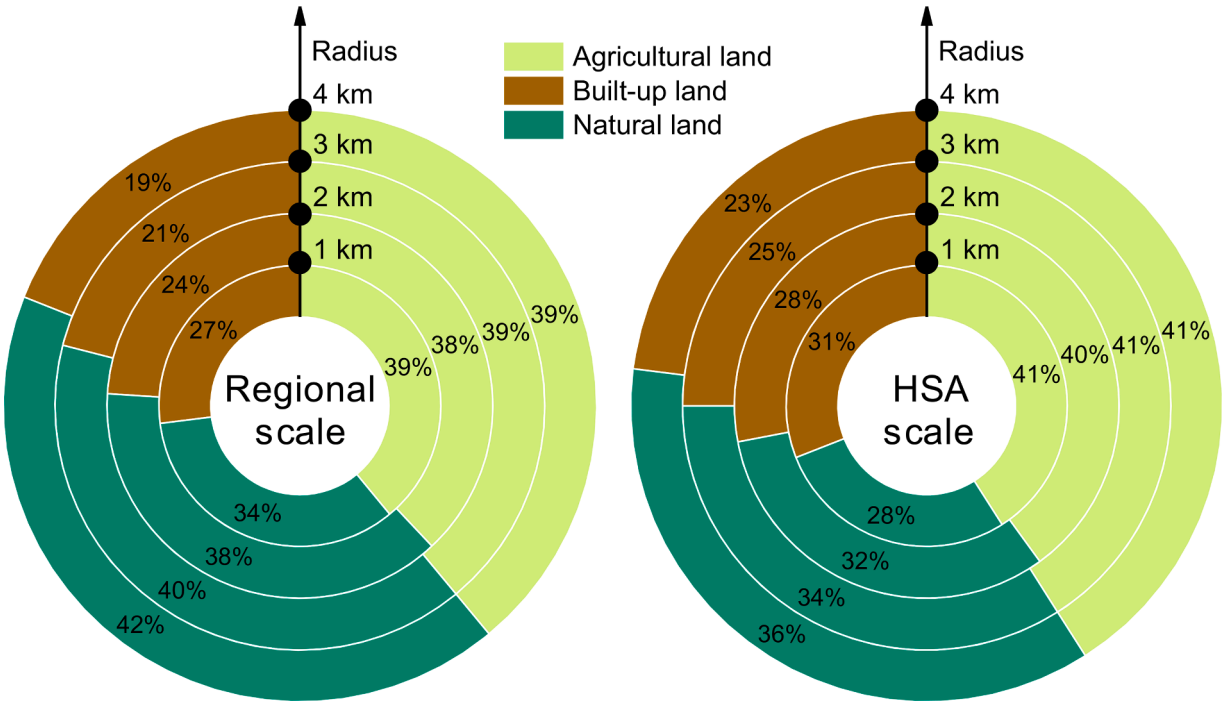

Fig. 4. Compositions of land use under different study radii and scales (n = 90). HSA, hydrologically sensitive area.

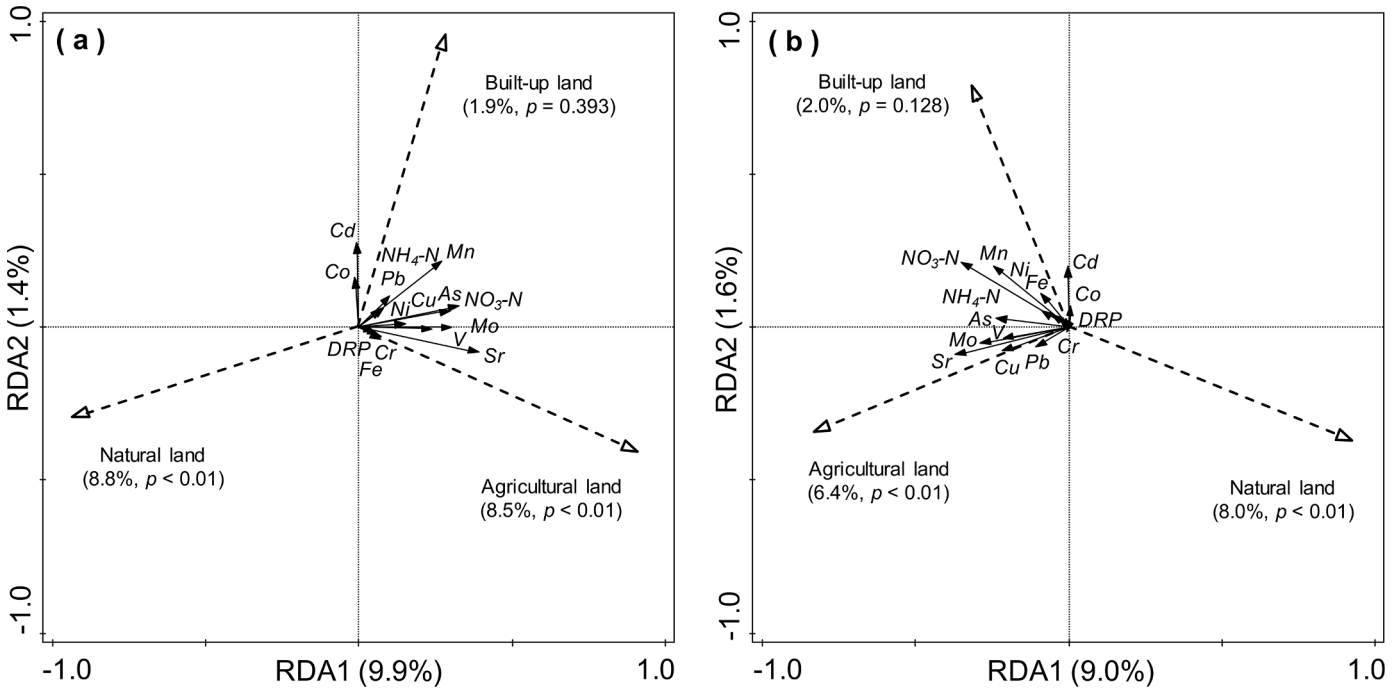

Fig. 5. Redundancy analysis (RDA) ordination plots of the relationship between land use and groundwater quality at the regional (a) and hydrologically sensitive area scales (b). The solid arrows with solid lines represent the response variables, while the hollow arrows with dashed lines represent explanatory variables. The positive and negative correlation between two variables are indicated by the same or opposite direction of the arrows, and the strength of correlation is proportional to the projection length of the arrows of the two variables. Numbers next to land use indicate the relative contribution rate of land use to groundwater quality. Numbers on the axis indicate the degree of explanation of the total variation.

the distance needs to be within a radius of 2 km for groundwater NO_3–N. Notably, lowering groundwater Cu requires a reduction in the agricultural area within a 3–km radius at the HSA scale (Table S8).

Overall, we highlight the key effects of land use composition within HSAs on groundwater quality at a national scale. The underlying mechanisms and the major pathways for these effects are fully summarized in the conceptual schematic (Fig. 6). We conclude that increasing the proportion of natural land and decreasing the proportion of both agricultural and built–up land at the HSA scale can significantly improve the river (Wang et al., 2023) and groundwater quality.

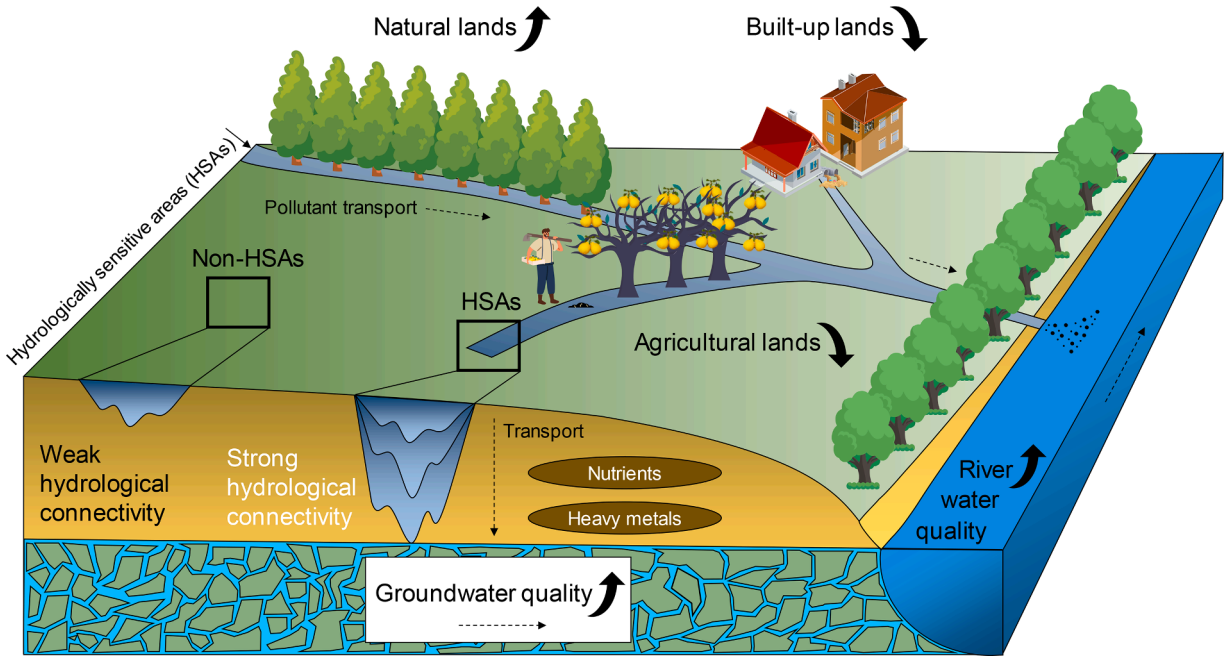

Fig. 6. Schematic showing the land management strategies based on hydrological connectivity to improve river water (Wang et al., 2023) and groundwater quality (this study).

3.3. Application

Over the past 60 years (1960–2019), global forest areas have experienced a net decrease of 81.7 million hectares due to intensive human activities (e.g., agricultural expansion and rapid urbanization) (Estoque et al., 2022). Human activities have also exacerbated the deterioration of the climate and soil and water around the world (Winkler et al., 2021). Afforestation (or "Grain for Green"), an important ecological restoration approach, has been widely reported to positively impact the global environment (Chen et al., 2019; Deng et al., 2017). However, which sites should be selected for planting trees/grass to alleviate the environmental crisis? Through this study, we firmly advocate that future ecological restoration should focus on the hydrological connectivity of terrestrial ecosystems, especially from the aspect of HSA regulations (e.g., the enhancement of natural land proportions) to improve groundwater and river quality. Here, we further discuss the feasibility of ecological restoration within HSAs to achieve a win–win solution between the environment and the economy.

(i) *Water storage*. Some studies have expressed concerns about soil and groundwater storage after afforestation (Feng et al., 2016; Jia et al., 2017; Li et al., 2018). However, it has also been shown that afforestation usually results in a limited decrease in the groundwater table. For example, Zhang and Hiscock (2010) indicate that afforestation will lead to a less than 0.3 m decline in the water table in the East Midlands, UK. HSAs are areas in watersheds that are highly prone to runoff generation due to soil saturation (Thomas et al., 2016). Therefore, compared with non–HSAs, HSAs are suitable sites that meet the water requirements of plants. The implementation of afforestation in HSAs will also minimally influence water storage.

(ii) *Soil erosion*. Anthropogenic–induced land use/cover change increases regional extreme climate events (Findell et al., 2017) and soil erosion (Borrelli et al., 2020). Forestland has a natural advantage in dealing with flooding and soil erosion. Spatially, HSAs have a high degree of consistency with 100–year floodplains (Qiu et al., 2020). Afforestation in HSAs showed a significant effect on reducing the concentrations of total suspended solids in rivers (Giri et al., 2018).

(iii) *Water quality and ecology*. Afforestation can weaken the hydrological connectivity of watersheds and reduce pollutant transfer (López-Vicente et al., 2016). Increasing the proportion of forestland within HSAs has a positive impact on the improvement of river water (Wang et al., 2023) and groundwater quality (this study). Qiu et al. (2019) indicated that the degradation of aquatic ecosystems can be alleviated by reducing human activities and protecting forest landscapes in HSAs.

(iv) *Biogeochemical cycles*. Previous research showed that the availability of soil organic carbon restricted microbial denitrification in the deep vadose zone (Chen et al., 2018). Afforestation contributed significantly to global soil carbon/nitrogen stocks (Li et al., 2012) and nutrient availability (Li et al., 2019). Afforestation in HSAs is expected to facilitate biogeochemical carbon/-nitrogen cycles and reduce nitrous oxide emissions (Deng et al., 2019). HSAs have high soil saturated water content, which greatly limits the penetration of oxygen, and thus facilitates denitrification (Zhu et al., 2018). Anderson et al. (2015) further indicated that the area of high STI value was usually accompanied by high denitrification rates ($R^2 = 0.86$).

(v) *Management investments*. HSAs usually account for approximately 20 % of the total watershed area (Zhou et al., 2022). Ecological restoration or pollution control in HSAs can significantly reduce investment in area management within a watershed (Thomas et al., 2016).

Currently, chemical oxidation, biodegradation, and adsorption are the major technologies for groundwater remediation (Zhang et al., 2017). However, the field application of these technical methods requires a large financial investment and faces great challenges due to complex environmental conditions. Recently, coupling human and natural systems in ecological restoration to achieve sustainable development has attracted increasing attention (Fu et al., 2023; Hannah et al., 2022). This is especially true from the perspective of land use management to improve water quality (Fernandes et al., 2021). The Outline of the National Land Greening Plan (2022–2030) indicates that China

plans to complete the greening of approximately 0.33 million km^2 in the following years. The above (i) to (v) aspects indicate the fact that HSAs are the priority areas for ecological restoration. Thus, we advocate prioritizing ecological restoration in HSAs to achieve harmony between the environment (improving groundwater quality) and the economy (reducing investment in area management).

3.4. Uncertainty analysis

Capturing the distribution of Ksat on a national scale is an enormous challenge (Vereecken et al., 2022). Here, the distribution of Ksat is based on the extrapolation of the RF model combined with geographic parameter (BD, clay, silty, and SOC) maps at the national scale. Usually, the national distributions of these geographic parameters are also obtained based on both field observations and model simulations. This may increase the uncertainty of Ksat in space. Thus, we further consider the distribution of HSAs without Ksat. By comparison, we find that the HSA distribution usually has a mean difference of 15.6 % (ranging from 0 to 37.4 %, n = 90) for both scenarios with and without considering Ksat (Fig. 7a). The difference % increases significantly with increasing mean slope and mean annual precipitation (p < 0.01) (Fig. 7b and c). This suggests that the hydrological connectivity is very sensitive to the spatial distribution of Ksat and should improve the Ksat prediction accuracy of in the future, especially in regions with high rainfall and steep terrain. Limited by computational power, we only extrapolated the distribution of Ksat within the sampling radius of 10 km (area= 314 km^2) according to research needs. Finally, approximately 26.7 million rows of Ksat data were obtained, which were further transformed into a raster of 30 m spatial resolution for HSA calculation. In the future, a national and even global map of the distribution of HSAs with a high spatial resolution will be necessary for pollution control and ecological restoration.

In the present study, groundwater sampling was mainly performed in the winter dry season, which reflects the relatively stable hydrological conditions. We found a significant impact of natural lands within HSAs on groundwater NO_3–N, Sr, Mo, Mn, and As (Table S7). Previous studies have shown that seasonal changes in rainfall can significantly alter hydrological processes (Mo et al., 2022; Yue et al., 2023). Hydrological connectivity may be more intense during the wet season, which further

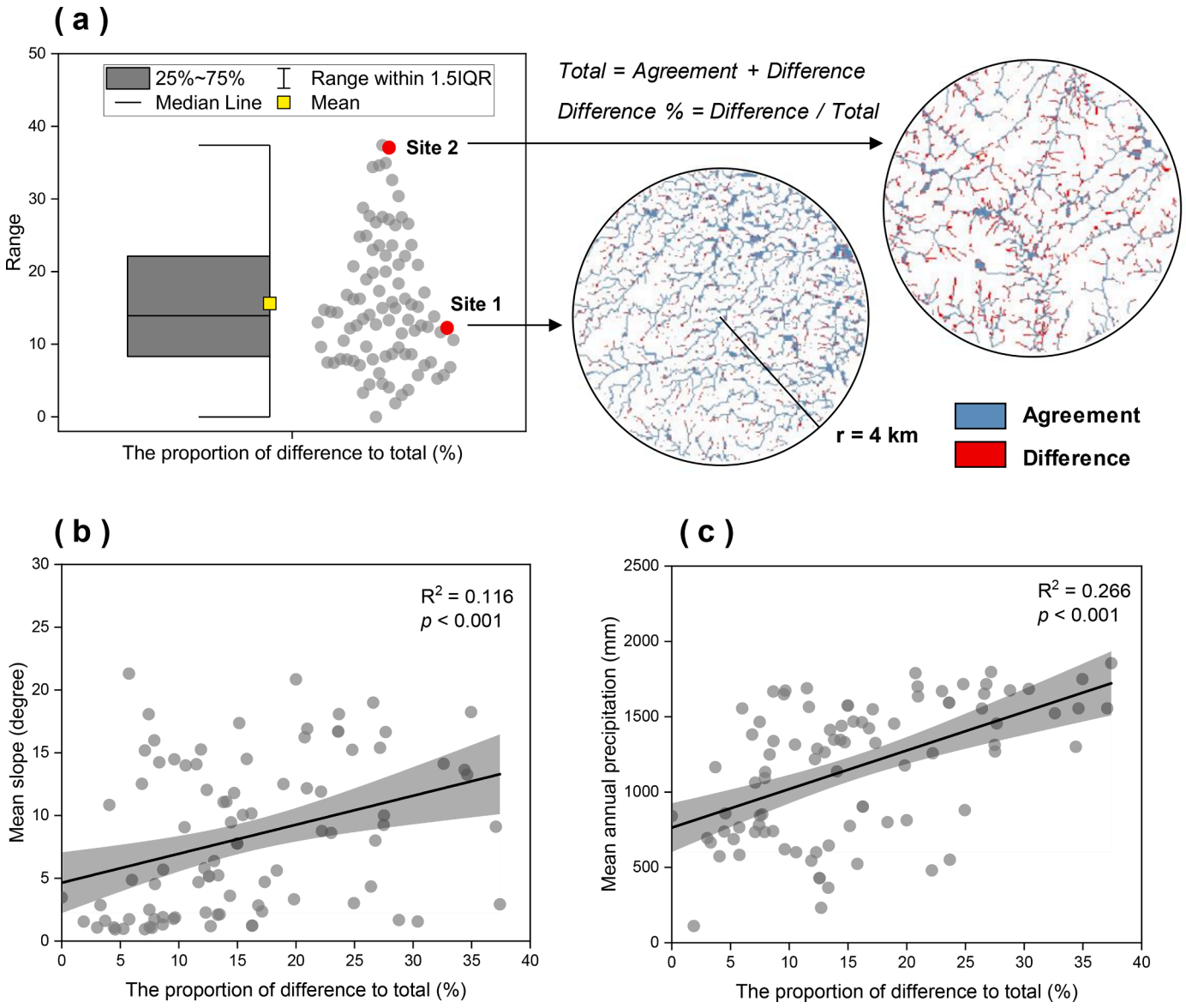

Fig. 7. Proportion of spatial difference for hydrologically sensitive areas when soil saturated hydraulic conductivity is considered or not (a), and how it relates to mean slope (b) and mean annual precipitation (c). Here, the locations of both site 1 and site 2 are shown in Fig. 1. The mean slope and mean annual precipitation (2016–2019, Table S1) are the mean values of the raster within a sampling radius of 4 km.

affects pollutant transport and groundwater quality (Good et al., 2015; Yue et al., 2023; Ebeling et al., 2021). In this study, groundwater collected at a depth of < 5 m had a higher NH_4–N concentration than that collected at > 5 m depth, but the opposite was true for groundwater NO_3–N (Table S5). Positively charged NH_4–N tends to be adsorbed by negatively charged humus and thus mainly exported via surface runoff, while negatively charged NO_3–N tends to be leached downwards to deeper saturation zones (Zhu et al., 2018). Mo et al. (2022) indicated that heavy rains promote the transfer of NH_4–N from the land surface to deep soil. More observations of groundwater over seasons are needed to explore the seasonal dynamics of hydrological processes and their effect on groundwater quality variation in the future.

The high heterogeneity of the vertical soil structure significantly alters the hydrological and material connections between land surface and groundwater (Oldham et al., 2013). This may promote a permanent or temporary hydrological and biogeochemical legacy in the deep vadose zone (Basu et al., 2022). Furthermore, such material legacies are regulated by retention times and reaction rates (Kolbe et al., 2019; Vautier et al., 2021; Severe et al., 2023). However, HSAs usually have strong hydrological connectivity, which may be frequently activated during rainfall events (Wang et al., 2023; Thomas et al., 2016). The influence of HSAs on groundwater quality may be less affected by time lag or material legacy caused by soil structure. In different years of groundwater sampling, we also found that the natural lands within HSAs had a positive impact on groundwater quality ($p < 0.05$ and $p < 0.01$), and the contribution was comparable to that at the regional scale (Table S6). Interdisciplinary studies integrating hydrogeology, pedology and biogeochemistry are still needed to address the lag and legacy issues in the process of pollutant transport from land to water.

4. Conclusions

We explored the effects of land use within HSAs on groundwater nutrients and heavy metals from the perspective of hydrological connectivity via nationwide survey and machine learning (random forest). Overall, the random forest model has good performance in extrapolating the distribution of Ksat and calculating HSAs at the national scale. HSAs occupied only approximately 20 % of the total land area, and their land use pattern explanation of the variability in groundwater quality is equivalent to that at the regional scale. Our study highlights the positive effects of increasing natural lands within HSAs on reducing groundwater nutrient and heavy metal concentrations in China. We therefore conclude that prioritizing ecological restoration in HSAs is conducive to achieving harmony between the environment and the economy.

CRediT authorship contribution statement

Yao Wang: Conceptualization, Data curation, Formal analysis, Investigation, Methodology, Validation, Visualization, Writing – original draft. **Yiqi Yu:** Formal analysis, Software, Validation. **Xin Luo:** Writing – review & editing. **Qiaoguo Tan:** Writing – review & editing. **Yuqi Fu:** Formal analysis. **Chenhe Zheng:** Investigation. **Deli Wang:** Data curation, Investigation, Writing – review & editing. **Nengwang Chen:** Data curation, Funding acquisition, Investigation, Supervision, Writing – review & editing.

Declaration of competing interest

The authors declare that they have no known competing financial interests or personal relationships that could have appeared to influence the work reported in this paper.

Data availability

Data will be made available on request.

Acknowledgments

This research was supported by the National Natural Science Foundation of China (51961125203) and the Fujian Province Water Conservancy Science and Technology Project (MSK202301; MSK202313). We thank three anonymous reviewers for their insightful comments and constructive suggestions that improved the manuscript. We thank Junou Du, Ting Lu, Yan Fang, Fan Qu and all the undergraduate and graduate students for their assistance in field investigation and lab analysis. Acknowledgment for the data support from "National Earth System Science Data Center, National Science & Technology Infrastructure of China (http://www.geodata.cn)".

Supplementary materials

Supplementary material associated with this article can be found, in the online version, at doi:10.1016/j.watres.2024.121247.

References

Anderson, T.R., Groffman, P.M., Walter, M.T., 2015. Using a soil topographic index to distribute denitrification fluxes across a northeastern headwater catchment. J. Hydrol. 522, 123–134.
Basu, N.B., Van-Meter, K.J., Byrnes, D.K., Van-Cappellen, P., Brouwer, R., Jacobsen, B.H., Jarsjö, J., Rudolph, D.L., Cunha, M.C., Nelson, N., Bhattacharya, R., Destouni, G., Olsen, S.B., 2022. Managing nitrogen legacies to accelerate water quality improvement. Nat. Geosci. 15, 97–105.
Borrelli, P., Robinson, D.A., Panagos, P., Lugato, E., Yang, J.E., Alewell, C., Wuepper, D., Montanarella, L., Ballabio, C., 2020. Land use and climate change impacts on global soil erosion by water (2015-2070). PNAS 117, 21994–22001.
Breiman, L., 2001. Random forests. Mach. Learn. 45, 5–32.
Chen, C., Park, T., Wang, X.H., Piao, S.L., Xu, B.D., Chaturvedi, R.K., Fuchs, R., Brovkin, V., Ciais, P., Fensholt, R., Tommervik, H., Bala, G., Zhu, Z.C., Nemani, R.R., Myneni, R.B., 2019. China and India lead in greening of the world through land-use management. Nat. Sustainability 2, 122–129.
Chen, S., Wang, F., Zhang, Y., Qin, S., Wei, S., Wang, S., Hu, C., Liu, B., 2018. Organic carbon availability limiting microbial denitrification in the deep vadose zone. Environ. Microbiol. 20, 980–992.
China updated nationally determined contributions. Climate Action Tracker, 2021. https://climateactiontracker.org/climate-target-update-tracker/china/.
Deng, L., Liu, S., Kim, D.G., Peng, C., Sweeney, S., Shangguan, Z., 2017. Past and future carbon sequestration benefits of China's grain for green program. Glob. Environ. Chang. 47, 13–20.
Deng, N., Wang, H., Hu, S., Jiao, J., 2019. Effects of afforestation restoration on soil potential N_2O emission and denitrifying bacteria after farmland abandonment in the Chinese Loess Plateau. Front. Microbiol. 10, 262.
Ebeling, P., Dupas, R., Abbott, B., Kumar, R., Ehrhardt, S., Fleckenstein, J.H., Musolff, A., 2021. Long-term nitrate trajectories vary by season in western European catchments. Global Biogeochem. Cycles 35.
Estoque, R.C., Dasgupta, R., Winkler, K., Avitabile, V., Johnson, B.A., Myint, S.W., Gao, Y., Ooba, M., Murayama, Y., Lasco, R.D., 2022. Spatiotemporal pattern of global forest change over the past 60 years and the forest transition theory. Environ. Res. Lett. 17.
Fan, T., Long, T., Lu, Y., Yang, L., Mi, N., Xia, F., Wang, X., Deng, S., Hu, Q., Zhang, F., 2022. Meta-analysis of Cd input-output fluxes in agricultural soil. Chemosphere 303, 134974.
Fatichi, S., Or, D., Walko, R., Vereecken, H., Young, M.H., Ghezzehei, T.A., Hengl, T., Kollet, S., Agam, N., Avissar, R., 2020. Soil structure is an important omission in Earth System Models. Nat. Commun. 11, 522.
Feng, X., Fu, B., Piao, S., Wang, S., Ciais, P., Zeng, Z., Lü, Y., Zeng, Y., Li, Y., Jiang, X., Wu, B., 2016. Revegetation in China's Loess Plateau is approaching sustainable water resource limits. Nat. Clim. Chang. 6, 1019–1022.
Fernandes, A.C.P., Martins, L.M.D.O., Pacheco, F.A.L., Fernandes, L.F.S., 2021. The consequences for stream water quality of long-term changes in landscape patterns: implications for land use management and policies. Land Use Policy 109.
Findell, K.L., Berg, A., Gentine, P., Krasting, J.P., Lintner, B.R., Malyshev, S., Santanello Jr., J.A., Shevliakova, E., 2017. The impact of anthropogenic land use and land cover change on regional climate extremes. Nat. Commun. 8, 989.
Fu, B., Liu, Y., Meadows, M.E., 2023. Ecological restoration for sustainable development in China. Natl. Sci. Rev. 10.
Ge, J., Zhang, Z., Lin, B., 2023. Towards carbon neutrality: how much do forest carbon sinks cost in China? Environ. Impact Assess. Rev. 98.
Giri, S., Qiu, Z.Y., Zhang, Z., 2017. A novel technique for establishing soil topographic index thresholds in defining hydrologically sensitive areas in landscapes. J. Environ. Manage. 200, 391–399.
Giri, S., Qiu, Z.Y., Zhang, Z., 2018. Assessing the impacts of land use on downstream water quality using a hydrologically sensitive area concept. J. Environ. Manage. 213, 309–319.
Good, S.P., Noone, D., Bowen, G., 2015. Hydrologic connectivity constrains partitioning of global terrestrial water fluxes. Science 349, 175–177.

Gu, B., Ge, Y., Chang, S.X., Luo, W., Chang, J., 2013. Nitrate in groundwater of China: sources and driving forces. Glob. Environ. Chang. 23, 1112–1121.
Gupta, S., Hengl, T., Lehmann, P., Bonetti, S., Or, D., 2021. SoilKsatDB: global database of soil saturated hydraulic conductivity measurements for geoscience applications. Earth Syst. Sci. Data 13, 1593–1612.
Hannah, D.M., Abbott, B.W., Khamis, K., Kelleher, C., Lynch, I., Krause, S., Ward, A.S., 2022. Illuminating the 'invisible water crisis' to address global water pollution challenges. Hydrol. Process 36.
He, S., Wu, J., Wang, D., He, X., 2022. Predictive modeling of groundwater nitrate pollution and evaluating its main impact factors using random forest. Chemosphere 290, 133388.
Jarsjo, J., Andersson-Skold, Y., Froberg, M., Pietron, J., Borgstrom, R., Lov, A., Kleja, D. B., 2020. Projecting impacts of climate change on metal mobilization at contaminated sites: controls by the groundwater level. Sci. Total Environ. 712, 135560.
Jia, X., Shao, M., Zhu, Y., Luo, Y., 2017. Soil moisture decline due to afforestation across the Loess Plateau, China. J. Hydrol. 546, 113–122.
Jiang, X.J., Chen, C.F., Zhu, X.A., Zakari, S., Singh, A.K., Zhang, W.J., Zeng, H.H., Yuan, Z.Q., He, C.G., Yu, S.Q., Liu, W.J., 2019. Use of dye infiltration experiments and HYDRUS-3D to interpret preferential flow in soil in a rubber-based agroforestry systems in Xishuangbanna, China. Catena 178, 120–131.
Kellner, E., Hubbart, J.A., Ikem, A., 2015. A comparison of forest and agricultural shallow groundwater chemical status a century after land use change. Sci. Total Environ. 529, 82–90.
Knoll, L., Breuer, L., Bach, M., 2020. Nation-wide estimation of groundwater redox conditions and nitrate concentrations through machine learning. Environ. Res. Lett. 15.
Koch, J., Stisen, S., Refsgaard, J.C., Ernstsen, V., Jakobsen, P.R., Hojberg, A.L., 2019. Modeling depth of the redox interface at high resolution at national scale using random forest and residual gaussian simulation. Water Resour. Res. 55, 1451–1469.
Kolbe, T., de Dreuzy, J.R., Abbott, B.W., Aquilina, L., Babey, T., Green, C.T., Fleckenstein, J.H., Labasque, T., Laverman, A.M., Marcais, J., Peiffer, S., Thomas, Z., Pinay, G., 2019. Stratification of reactivity determines nitrate removal in groundwater. Proc. Natl. Acad. Sci. USA 116, 2494–2499.
Leibowitz, S.G., Hill, R.A., Creed, I.F., Compton, J.E., Golden, H.E., Weber, M.H., Rains, M.C., Jones Jr., C.E., Lee, E.H., Christensen, J.R., Bellmore, R.A., Lane, C.R., 2023. National hydrologic connectivity classification links wetlands with stream water quality. Nat. Water 1, 370–380.
Li, B., Yang, G., Wan, R., Hörmann, G., Huang, J., Fohrer, N., Zhang, L., 2017. Combining multivariate statistical techniques and random forests model to assess and diagnose the trophic status of Poyang Lake in China. Ecol. Indic. 83, 74–83.
Li, C., Li, C., Zhao, L., Ma, Y., Tong, X., Deng, J., Ren, C., Han, X., Yang, G., 2019. Dynamics of storage and relative availability of soil inorganic nitrogen along revegetation chronosequence in the loess hilly region of China. Soil Tillage Res. 187, 11–20.
Li, D., Niu, S., Luo, Y., 2012. Global patterns of the dynamics of soil carbon and nitrogen stocks following afforestation: a meta-analysis. New Phytol. 195, 172–181.
Li, J., Li, Z., Brandis, K.J., Bu, J., Sun, Z., Yu, Q., Ramp, D., 2020. Tracing geochemical pollutants in stream water and soil from mining activity in an alpine catchment. Chemosphere 242, 125167.
Li, L., Qiao, J., Yu, G., Wang, L., Li, H.Y., Liao, C., Zhu, Z., 2022. Interpretable tree-based ensemble model for predicting beach water quality. Water Res. 211.
Li, S., Cai, X., Niroula, S., Wallington, K., Gramig, B.M., Cusick, R.D., Singh, V., McIsaac, G., Oh, S., Kurambhatti, C., Emaminejad, S.A., John, S., 2023. Integrated agricultural practices and engineering technologies enhance synergies of food-energy-water systems in corn belt watersheds. Environ. Sci. Technol. 57, 9194–9203.
Li, Y., Piao, S.L., Li, L.Z.X., Chen, A.P., Wang, X.H., Ciais, P., Huang, L., Lian, X., Peng, S. S., Zeng, Z.Z., Wang, K., Zhou, L.M., 2018. Divergent hydrological response to large-scale afforestation and vegetation greening in China. Sci. Adv. 4.
Liang, C.P., Lin, T.C., Suk, H., Wang, C.H., Liu, C.W., Chang, T.W., Chen, J.S., 2022. Comprehensive assessment of the impact of land use and hydrogeological properties on the groundwater quality in Taiwan using factor and cluster analyses. Sci. Total Environ. 851, 158135.
Liu, Z., Deng, Z., He, G., Wang, H., Zhang, X., Lin, J., Qi, Y., Liang, X., 2021. Challenges and opportunities for carbon neutrality in China. Nat. Rev. Earth Environ. 3, 141–155.
López-Vicente, M., Nadal-Romero, E., Cammeraat, E.L.H., 2016. Hydrological connectivity does change over 70 years of abandonment and afforestation in the spanish pyrenees. Land Degradation Develop. 28, 1298–1310.
McDonough, L.K., Santos, I.R., Andersen, M.S., O'Carroll, D.M., Rutlidge, H., Meredith, K., Oudone, P., Bridgeman, J., Gooddy, D.C., Sorensen, J.P.R., Lapworth, D.J., MacDonald, A.M., Ward, J., Baker, A., 2020. Changes in global groundwater organic carbon driven by climate change and urbanization. Nat. Commun. 11, 1279.
Mihiranga, H.K.M., Jiang, Y., Li, X., Wang, W., De-Silva, K., Kumwimba, M.N., Bao, X., Nissanka, S.P., 2021. Nitrogen/phosphorus behavior traits and implications during storm events in a semi-arid mountainous watershed. Sci. Total Environ. 791, 148382.
Mitchell, E., Frisbie, S., Sarkar, B., 2011. Exposure to multiple metals from groundwater-a global crisis: geology, climate change, health effects, testing, and mitigation. Metallomics 3, 874–908.
Mo, X., Peng, H., Xin, J., Wang, S., 2022. Analysis of urea nitrogen leaching under high-intensity rainfall using HYDRUS-1D. J. Environ. Manage. 312, 114900.
Oldham, C.E., Farrow, D.E., Peiffer, S., 2013. A generalized Damkohler number for classifying material processing in hydrological systems. Hydrol. Earth Syst. Sci. 17, 1133–1148.
Qiu, Z., Lyon, S.W., Creveling, E., 2020. Defining a topographic index threshold to delineate hydrologically sensitive areas for water resources planning and management. Water Resour. Manage. 34, 3675–3688.
Qiu, Z.Y., Kennen, J.G., Giri, S., Walter, T., Kang, Y., Zhang, Z., 2019. Reassessing the relationship between landscape alteration and aquatic ecosystem degradation from a hydrologically sensitive area perspective. Sci. Total Environ. 650, 2850–2862.
Scanlon, B.R., Fakhreddine, S., Reedy, R.C., Yang, Q., Malito, J.G., 2022. Drivers of spatiotemporal variability in drinking water quality in the United States. Environ. Sci. Technol. 56, 12965–12974.
Schilling, K.E., Jacobson, P.J., Vogelgesang, J.A., 2015. Agricultural conversion of floodplain ecosystems: implications for groundwater quality. J. Environ. Manage. 153, 74–83.
Severe, E., Errigo, I.M., Proteau, M., Sayedi, S.S., Kolbe, T., Marçais, J., Thomas, Z., Petton, C., Rouault, F., Vautier, C., deDreuzy, J.R., Moatar, F., Aquilina, L., Wood, R. L., LaBasque, T., Lécuyer, C., Pinay, G., Abbott, B.W., 2023. Deep denitrification: stream and groundwater biogeochemistry reveal contrasted but connected worlds above and below. Sci. Total Environ. 880.
Tang, W., Xu, Y.J., Ni, M., Li, S., 2023. Land use and hydrological factors control concentrations and diffusive fluxes of riverine dissolved carbon dioxide and methane in low-order streams. Water Res. 231, 119615.
Thomas, I.A., Jordan, P., Mellander, P.E., Fenton, O., Shine, O., HUallachain, D.O., Creamer, R., McDonald, N.T., Dunlop, P., Murphy, P.N.C., 2016. Improving the identification of hydrologically sensitive areas using LiDAR DEMs for the delineation and mitigation of critical source areas of diffuse pollution. Sci. Total Environ. 556, 276–290.
Vautier, C., Kolbe, T., Babey, T., Marcais, J., Abbott, B.W., Laverman, A.M., Thomas, Z., Aquilina, L., Pinay, G., de Dreuzy, J.R., 2021. What do we need to predict groundwater nitrate recovery trajectories? Sci. Total Environ. 788.
Vereecken, H., Amelung, W., Bauke, S.L., Bogena, H., Bruggemann, N., Montzka, C., Vanderborght, J., Bechtold, M., Bloschl, G., Carminati, A., Javaux, M., Konings, A.G., Kusche, J., Neuweiler, I., Or, D., Steele-Dunne, S., Verhoef, A., Young, M., Zhang, Y. G., 2022. Soil hydrology in the earth system. Nat. Rev. Earth Environ. 3, 573–587.
Wang, D.L., Lin, W.F., Yang, X.Q., Zhai, W.D., Dai, M.H., Chen, C.T.A., 2012. Occurrences of dissolved trace metals (Cu, Cd, and Mn) in the Pearl River Estuary (China), a large river-groundwater-estuary system. Cont. Shelf Res. 50-51, 54–63.
Wang, H., Yan, S., Ciais, P., Wigneron, J.P., Liu, L., Li, Y., Fu, Z., Ma, H., Liang, Z., Wei, F., Wang, Y., Li, S., 2022. Exploring complex water stress-gross primary production relationships: impact of climatic drivers, main effects, and interactive effects. Glob. Chang. Biol. 28, 4110–4123.
Wang, Y., Lin, J., Wang, F., Tian, Q., Zheng, Y., Chen, N., 2023. Hydrological connectivity affects nitrogen migration and retention in the land-river continuum. J. Environ. Manage. 326.
Winkler, K., Fuchs, R., Rounsevell, M., Herold, M., 2021. Global land use changes are four times greater than previously estimated. Nat. Commun. 12, 2501.
Yang, S., Feng, W., Wang, S., Chen, L., Zheng, X., Li, X., Zhou, D., 2021. Farmland heavy metals can migrate to deep soil at a regional scale: a case study on a wastewater-irrigated area in China. Environ. Pollut. 281, 116977.
Yuan, L., Fei, W., Jia, F., Junping, L., Qi, L., Fangru, N., Xudong, L., Lan, X., Shulian, X., 2020. Increased health threats from land use change caused by anthropogenic activity in an endemic fluorosis and arsenicosis area. Environ. Pollut. 261, 114130.
Yue, F.J., Li, S.L., Waldron, S., Oliver, D.M., Chen, X., Li, P., Peng, T., Liu, C.Q., 2023. Source availability and hydrological connectivity determined nitrate-discharge relationships during rainfall events in karst catchment as revealed by high-frequency nitrate sensing. Water Res. 231, 119616.
Xie, X., Pu, L., Zhu, M., Meadows, M., Sun, L., Wu, T., Bu, X., Xu, Y., 2021. Differential effects of various reclamation treatments on soil characteristics: an experimental study of newly reclaimed tidal mudflats on the east China coast. Sci. Total Environ. 768, 144996.
Xu, Y., Li, K., Liu, Y., Liu, Z., Wang, L., Pu, J., Xu, Z., Sun, H., 2019. Combined effects of artificial sweetener acesulfame on the uptake of Cd in rice (Oryza sativa L.). Environ. Pollut. 252, 171–179.
Zhang, H., Hiscock, K.M., 2010. Modelling the impact of forest cover on groundwater resources: a case study of the Sherwood Sandstone aquifer in the East Midlands, UK. J. Hydrol. 392, 136–149.
Zhang, S., Mao, G., Crittenden, J., Liu, X., Du, H., 2017. Groundwater remediation from the past to the future: a bibliometric analysis. Water Res. 119, 114–125.
Zhou, Y., Deng, J., Li, Z., Wang, T., Du, Y., Zhao, S., Zhang, X., 2022. Targeting the critical source areas of phosphorus based on hydrological sensitive area delineation to control nonpoint source pollution in watersheds. Front. Environ. Sci. 10.
Zhu, Q., Castellano, M.J., Yang, G., 2018. Coupling soil water processes and the nitrogen cycle across spatial scales: potentials, bottlenecks and solutions. Earth Sci. Rev. 187, 248–258.